Swelling of Transported Smoke from Savanna fires over the Southeast Atlantic Ocean?

J. Kar[1,2], M. Vaughan[2], J. Tackett[1,2], Z. Liu[2], A. Omar[2], S. Rodier[1,2], C. Trepte[2], P. Lucker[1]

[1] Science Systems and Applications Inc., Hampton, VA

[2] NASA Langley Research Center, Hampton, VA

Abstract.

We use the recently released Version 4 (V4) lidar data products from CALIPSO to study the smoke plumes transported from Southern African biomass burning areas. The significant improvements in CALIPSO V4 Level 1 calibration and the V4 Level 2 aerosol subtyping algorithms, the latter being particularly relevant to biomass burning smoke over this area, lead to a better representation of their optical properties. For the first time, we show evidence of smoke particles increasing in size, evidenced in their particulate color ratios, as they are transported over the South Atlantic Ocean from the source regions over Southern Africa. This is likely due to hygroscopic swelling of the smoke particles and is reflected in the higher relative humidity in the middle troposphere for profiles with smoke. This finding may have implications for radiative forcing estimates over this area and is relevant to the ORACLES field mission that is currently underway.

Key points:

1. Optical properties of smoke particles transported over Southeast Atlantic Ocean studied using CALIPSO lidar data (V4).

2. Size of the smoke particles shows a distinct increase from land to ocean.

3. This is likely due to hygroscopic swelling as seen in the relative humidity profiles.

1. Introduction:

The impact of different types of aerosols on our environment is not very well understood and there is an ever-increasing need to characterize the various aerosol types in different parts of the globe (IPCC, 2013). In particular, the smoke from biomass burning needs to be understood better because of the important radiative effects of black carbon (Bond et al., 2013), and because forest fires have been growing in size and frequency in many parts of the world. As such, there have been many studies of biomass burning smoke and their properties and evolution with time (e.g., Reid et al., 2005, Semeniuk et al., 2007, Saide et al., 2015) and some of these properties depend upon the location and type of burning, e.g., smoldering or flaming.

Over Southern Africa, savanna burning occurs every year between June and October and constitutes the largest source of biomass burning smoke over the globe (IPCC, 2013; Van der Werf et al., 2010). The smoke plumes from these fires get transported over the Southeast Atlantic Ocean over 5-7 days, overlaying one of the largest low altitude extended stratus cloud decks anywhere on the globe, which has consequences for radiative forcing estimates in this area. Passive satellite remote sensing has limited utility for studying these plumes, and vertically resolved information on these “above cloud aerosols” (ACA) is crucial. This vertical information has become possible in the last decade because of the space borne lidar CALIPSO, which has been providing high quality measurements of the aerosol vertical profiles globally since June 2006 (Winker et al., 2009). Measurements from CALIPSO have been used to derive highly accurate estimates of radiative forcing of the ACA in this region (Chand et al., 2008, 2009).

In the CALIPSO data processing sequence, the attenuated backscatter data are first examined to detect the layers using a thresholding algorithm (Vaughan et al., 2009) and then the layers are classified as either a cloud or aerosol (Liu et al., 2009). The aerosol layers are subsequently assigned various subtypes based on their optical properties and geospatial location (Omar et al., 2009). The November 2016 release of version 4.1 (V4) of the CALIPSO Level 2 lidar data products incorporates significant improvements in the retrieval algorithms, including the subtype assignments. In particular, there was a significant anomaly in the subtyping over the Southeast Atlantic in earlier versions, where many smoke layers were misclassified as marine layers. This has since been addressed in V4. Many more smoke layers are now identified over the Atlantic, thus presenting a good opportunity for further study of these extensive and regularly occurring smoke plumes. In particular, the evolution of the optical properties of these smoke plumes as they are transported to great distances over the South Atlantic may now be better characterized.

In this letter, we use V4 CALIPSO data to present evidence of the evolution of size of the smoke particles being exported from the Southern African savanna burning zones. We show that these particles tend to increase in size as they are transported over large distances over the ocean. While most constituents of smoke plumes are generally hydrophobic, aging and oxidation processes during the transport might make them hydrophilic, and the signatures of this behavior could be discerned in the relative humidity data. This result should be of interest to the currently ongoing Observations of Aerosols above Clouds and their Interactions (ORACLES) aircraft mission studying the smoke and its interaction with clouds over the same area (Zuidema et al., 2016).

2. Data:

We use the CALIPSO V4 level 2 aerosol profile product, which reports height-resolved profiles of the total backscatter and extinction coefficients at 532 nm and 1064 nm as well as the perpendicular backscatter coefficients at 532 nm for all layers detected. The horizontal resolution of the data is 5km while the vertical resolution is 60m up to 20km and 180m above that. As part of the V4 level 2 updates, the retrieval algorithms were optimized to take maximum advantage of the changes in the V4 level 1 data which were released earlier, with significant improvements in both the 532 nm and 1064 nm channel calibrations (Getzewich et al., 2015). In particular, the improvement in 1064 nm channel calibration makes it feasible to study the color ratio (ratio of backscatter at 1064 nm to that at 532 nm) with a higher degree of confidence in this new data set. We use smoke subtypes for our analysis. Previous iterations of the CALIPSO aerosol subtype assignments have been validated by comparison with AERONET data as well as high spectral resolution lidar (HSRL) data (Mielonen et al., 2009, Misra et al., 2013, Burton et al., 2013, Bibi et al., 2016). We also use the 1064 nm measurements retrieved from the Cloud-Aerosol Transport System (CATS) lidar on board the International Space Station (ISS) Mode 7.2 Version 1-05 level 2 Operational (L2O) Layer and Profile data products. The CATS lidar measures 1064 nm elastic backscatter in polarization planes parallel and perpendicular to the transmitted linearly polarized laser pulses, thus providing depolarization ratio data at 1064 nm since March 2015 (Yorks et al., 2016).

3. Results

3.1. Particulate color ratio evolution in transported smoke.

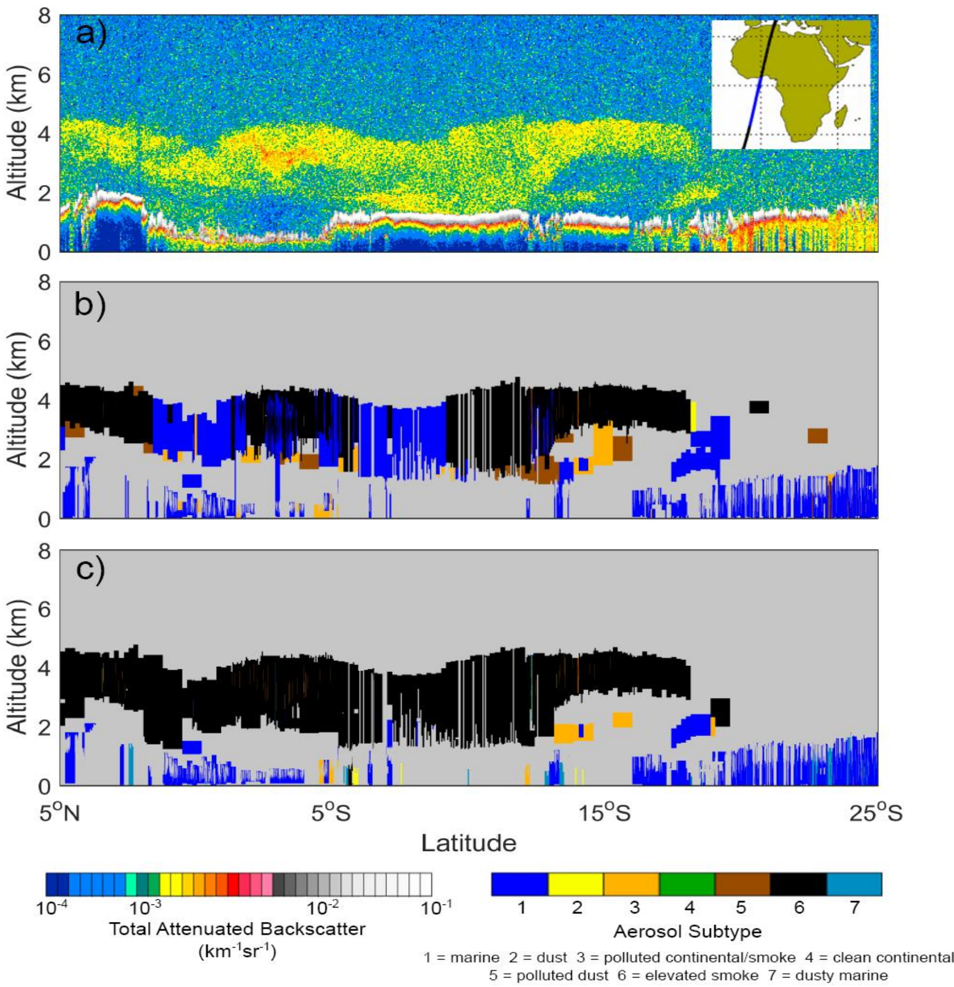

Figure 1. CALIPSO browse images of a) 532 nm attenuated backscatter coefficients and b) aerosol subtypes from V3 and c) V4 on September 5, 2010.

Figure 1a shows the 532 nm attenuated backscatter coefficients measured over the South Atlantic off the coast of Southern Africa on September 5, 2010. The extended plume at 2-5 km altitude between 19^{o}S and 5^{o}N is smoke that has been transported from the extensive fires that occur over Southern Africa between June and October every year. Figure 1b shows the aerosol subtypes assigned in the version 3 (V3) data products. As can be seen, in the V3 analysis the plume between 2 and 5 km is punctuated by a large number of misclassified marine layers (in blue). The misclassification of smoke layers as marine was a pervasive problem in V3 data over this area. Figure 1c shows the recently released V4 data, where now we can see a fuller and more coherent smoke plume. The V4 analysis reports much larger number of smoke layers (and an upward revision of the aerosol optical depth) over this most important and extensive biomass burning area. Thus, we now have more representative information about the spatial extent of biomass burning plumes in this region so that we can better exploit the optical properties reported in the CALIPSO data products.

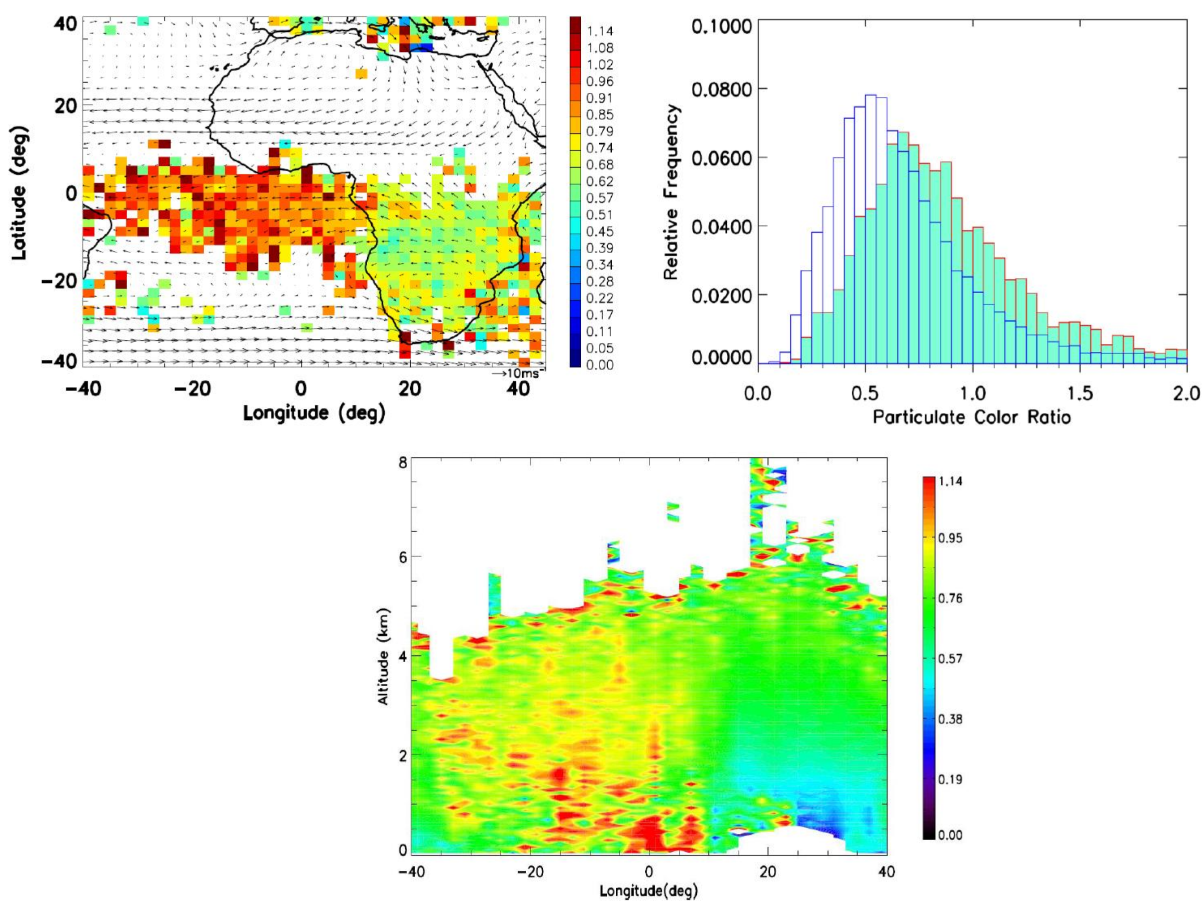

Figure 2. a) Particulate color ratio distribution of smoke at 3.03 km for August, 2006-2010 (binned at 2^{o}x2^o in latitude and longitude), with wind vectors from MERRA-2 (August 2006-2010) re-binned into 2.5^{o}x2.5^o in latitude and longitude; b) histograms of particulate color ratio over land (25^{o}S-0,10^{o}E-35^{o}E, in blue) and ocean (25^{o}S-0, 30^{o}W-10^{o}E, in aquamarine, filled) at 3.03 km (August 2006-2010); and c) height-longitude cross section of particulate color ratio along 0-25^{o}S (August 2006-2010).

Figure 2a shows the spatial distribution of the particulate color ratio of the aerosol samples classified as smoke at 3.03 km using nighttime data for the month of August averaged over 2006-2010. An important change in CALIPSO V4 that is particularly relevant over this area is that the V4 aerosol subtyping algorithm no longer distinguishes between polluted continental and smoke at low altitudes. Instead these layers are identified as “polluted continental/smoke”. An “elevated smoke” subtype is defined for those smoke layers with top altitudes exceeding 2.5 km. We have included both smoke categories in our analysis. The particulate color ratio is the ratio of the total backscatter coefficients at 1064 nm and 532 nm, and provides a measure of aerosol particle size. The data shown in Figure 2 used only cloud free nighttime profiles. Further, we have included data from only those profiles which had the extinction quality control flag as either zero, indicating that the initial lidar ratio resulted in stable extinction retrievals, or one, which flags those cases where the lidar ratio could be inferred directly from the data (constrained retrievals). We also filtered out the data points where the extinction uncertainty estimate diverged and where the uncertainty of particulate color ratio exceeds 500%. A minimum number of 15 samples was used for each grid box.

As can be seen in Figure 2a, there is a clear increase in the particulate color ratio values from the source areas over land to those over the ocean. Figure 2b shows the histograms of the particulate color ratio at 3.03 km over the source regions on land (in blue, between 25^{o}S-equator, 10^{o}E-35^{o}E) and over oceanic regions (in aquamarine, filled, between 25^{o}S-equator, 30^{o}W-10^{o}E). There is a significant difference in the color ratio distribution between land and ocean. At 3.03 km, the mean particulate color ratio over land is ~0.7 while that over the ocean is ~0.9, an increase of ~29%, while at 2 km it can be as much as 60% with much larger contrast in the color ratio distributions between land and ocean (not shown). This likely represents an increase in the size of the smoke particles as they are swept over the ocean over 5-7 days. To our knowledge this is the first time such an increase in the size of the smoke particles is being reported over this area. This was seen for all months between June and October and in all years with some interannual variability. Similar results were also obtained using the daytime data. The full altitude information can be seen in Figure 2c, which shows the height-longitude cross-section of the particulate color ratios over 0-25^{o}S, using only the cloud free nighttime profiles for August 2006-2010. Once again, the difference between the land and ocean can be clearly seen with somewhat higher values at the lowest altitudes over the ocean, which might be due to gravitational settling of relatively larger and heavier particles. Given that this phenomenon occurs consistently for the key biomass burning months every year, it is not likely to be a data artifact.

The current version (V4.10) of CALIPSO data processing scheme employs the Modern Era Retrospective Analysis for Research and Applications version 2 (MERRA-2) for meteorological information. The latter, for the first time, assimilates aerosol optical depth (AOD) retrieved from AVHRR, MODIS, MISR and AERONET through the integration of the GOCART model and the aerosol radiative feedbacks to the atmospheric fields (Randles et al., 2016). Comparisons of MERRA-2 assimilated AODs with independent retrievals (including DIAL/HSRL from SEAC^{4}RS) have shown good correlations. The vertical profiles of the total attenuated backscatter from MERRA-2 generally reproduce the CALIPSO vertical profiles at various places over the globe but show some biases (Randles et al., 2016). Insofar as MERRA-2 already incorporates aerosol information, it is important to determine if the results presented above are biased in any way. We found similar particulate color ratio enhancements over the ocean using V3 CALIPSO data, which reported fewer smoke layers but used GEOS-5.7.2 meteorological data that did not assimilate the aerosol information, thus discounting the possibility of any bias coming from the MERRA-2 meteorology.

3.2 Relative Humidity Variations

The most likely explanation for the increase in size of the smoke particles has to do with swelling of the particles by water uptake which might have a signature in the relative humidity (RH) profiles.

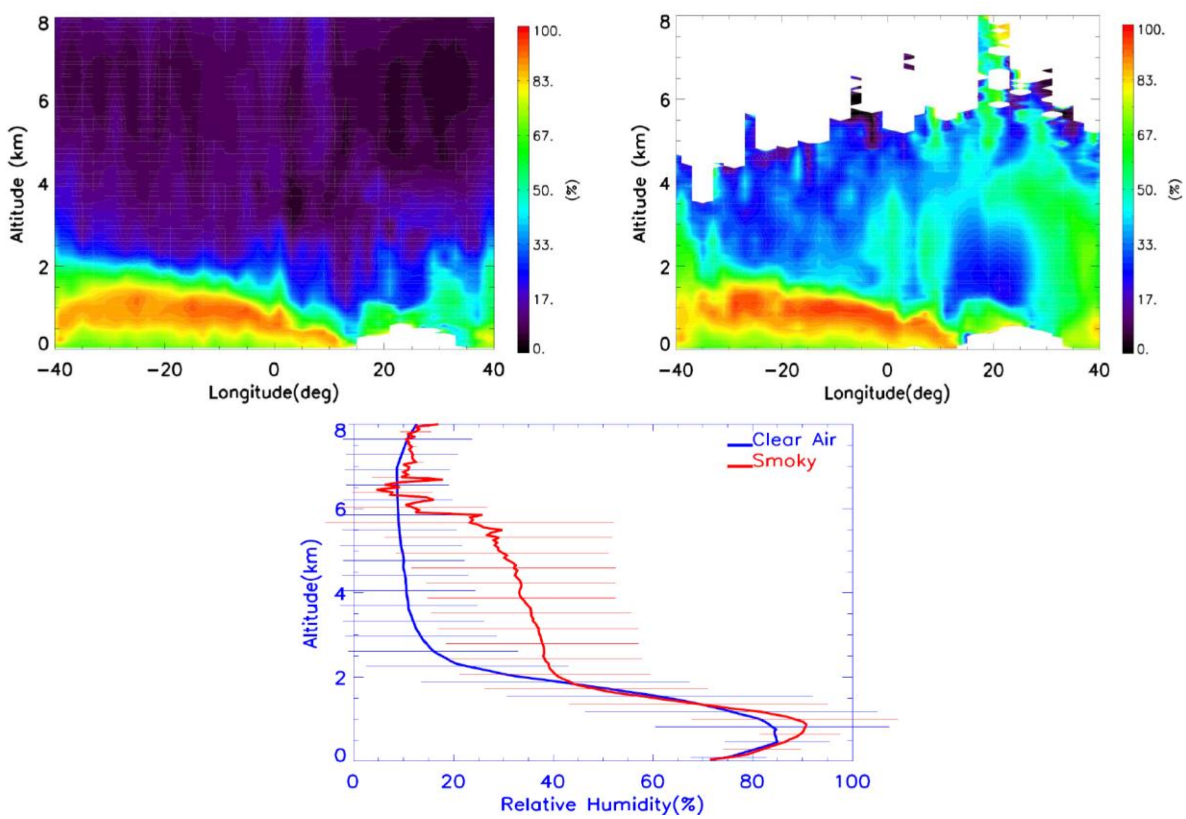

Figure 3. Height longitude cross sections (0-25^{o}S) of relative humidity for a) clear air profiles, b) profiles with smoke samples in them, and c) averaged profiles and standard deviations of relative humidity (0-25^{o}S, 30^{o}W-10^{o}E, using all data for August, 2006-2010.

Figures 3a and 3b show the height longitude distribution of RH from MERRA-2 as available in CALIPSO data files averaged over 25°S-equator, for August 2006-2010 nighttime data. The clear air RH profiles correspond to cloud free and aerosol free columns within this area, while the smoky profiles correspond to columns that are cloud free but contain smoke samples (essentially corresponding to Fig 2c). Enhanced RH values seem to be associated with the biomass burning smoke plumes. As can be seen in Figure 3c, there is a notable difference between the two mean RH profiles between 2 km and 6 km (over the Atlantic ocean, 0-25^{o}S, 30^{o}W-10^{o}E) where the RH values for the smoky profile are substantially larger than in the clear air mean profile.

To characterize the uncertainty in MERRA RH profiles, Adebiyi et al. (2015) had earlier shown that the RH profiles on average tend to reproduce the large scale features from high resolution radiosonde profiles obtained at St. Helena Island (~16°S, 6°W), which is located near the southern parts of the region in this study. The deviation in the mean RH profiles between MERRA and radiosondes is ~10% (Adebiyi et al., 2015). However the bias changes sign around 700 hPa. Below this pressure level, MERRA profiles have a low bias as compared to sondes; above this pressure level, they have a higher bias. Note, however, that Adebiyi et al. (2015) used an earlier version of the MERRA product, and not the MERRA-2 reanalyses.

The mid-tropospheric difference between the smoky and the clear air RH profiles in Figure 3c is quite similar to the results of Adebiyi et al. (2015) at St. Helena Island, representing the difference between polluted and non-polluted conditions. The increase in moisture collocated with increased aerosol loading suggests an environment conducive for swelling of smoke particles as evidenced by the increase in particulate color ratio. There is also large variability in the RH profiles for the smoke samples. Adebiyi et al. (2015) presented individual CALIPSO smoke extinction profiles which often closely matched that of the radiosonde RH profiles at St. Helena with high RH values (~ 80%) at the top of the smoke layer with the largest extinctions. In contrast, the RH profiles for the non-smoke days showed much lower RH values (≤ 20%) in the mid troposphere. Adebiyi et al. (2015) do not discuss the possible swelling effects on the smoke particles, though they do mention the possibility of this occurring.

3.3. Particulate depolarization of smoke

Is there any other evidence of swelling of the smoke particles due to water uptake, as, for example, in their shape? The particulate depolarization ratio (i.e., the ratio of the backscatter in the perpendicular and parallel channels at 532 nm) reported in the CALIPSO data provides insight into the shape of the scattering particles. In general, swelling might be expected to enhance the sphericity of particles. However, because biomass burning typically generates quasi-spherical particles having low depolarization ratios (Burton et al., 2013), it may be difficult to detect further changes in particle shape using this measurement.

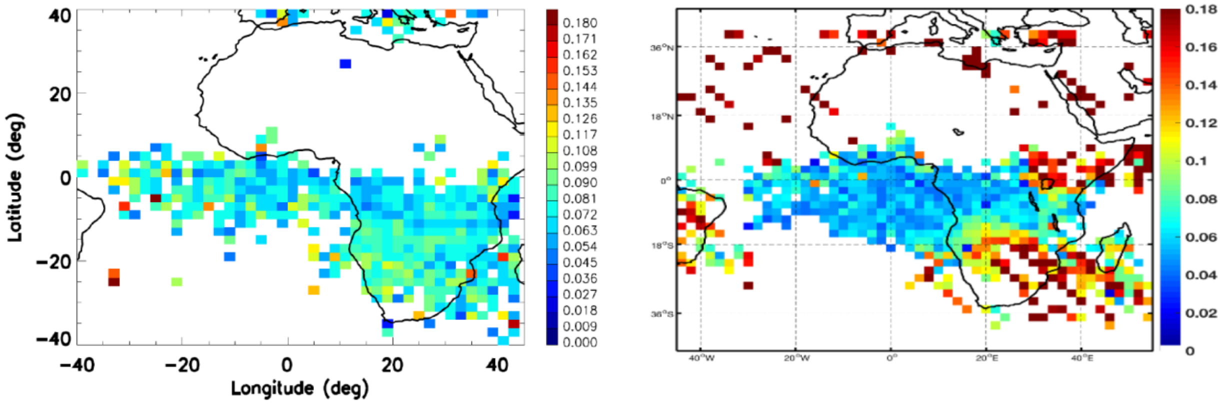

Figure 4. a) Particulate depolarization of smoke at 532 nm at 3.03 km from CALIPSO for August, 2006-2010 and b) volume depolarization of smoke at 1064 nm at 3 km from CATS for August 2015-2016. A minimum number of 15 samples per grid box was used for each plot.

Figure 4a shows the spatial distribution of the particular depolarization of smoke samples at 3.03 km from CALIPSO, once again using only nighttime cloud free profiles in August for 2006-2010. We rejected depolarization data having estimated relative uncertainty above 500%. This criterion removes data points with very low negative particulate depolarization with associated uncertainties much higher than 500%. There is significant noise in the data. There seems to be suggestion of a somewhat higher depolarization over the land areas over South Africa as compared to the oceanic regions, although the contrast is not as striking as the particulate color ratios shown in Figure 2. As an independent measurement, Figure 4b shows the spatial distribution of the volume depolarization of smoke at 3 km at 1064 nm as observed by the CATS lidar for August 2015-2016. The CATS data products do not report particulate depolarization ratios. However, because molecular contributions to the backscatter signal at 1064 nm are substantially smaller than at 532 nm (by a factor of ~17), the CATS 1064 nm volume depolarization ratios should provide essentially the same information as the particulate depolarization ratios. The CATS depolarization ratios also show somewhat higher values over the source regions and fall off to somewhat lower values over the Atlantic Ocean. Note that CATS data products are only available at 1064 nm, so we cannot confirm the changing color ratio using the CATS data.

4. Discussion and Conclusions:

We have presented evidence of an increase in the size of smoke particles that are transported over the South Atlantic Ocean in large amounts from the biomass burning regions of South Africa as reflected in the particulate color ratios retrieved from the CALIPSO space borne lidar. Coagulation may be ruled out as a possible cause of this result so far away from the emission regions, although Radke et al. (1995) found significant changes in smoke size distributions in a large plume from Oregon and suggested these could be occurring due to coagulation. On the other hand, the enhanced RH profiles for smoke samples in the mid troposphere as compared to the clear air samples suggests an association with water uptake by these particles. As such, there have been reports of significantly increased moisture content in biomass burning smoke plumes, particularly for smoldering fires (Achtemeir, 2006, Clements et al., 2006). In Southern Africa, smoldering fires may be more frequent towards the equator during the wet season (Midzak et al., 2017). A number of studies have confirmed the hygroscopicity of smoke under certain conditions. Semeniuk et al. (2007) studied the hygroscopic behavior of 80 aerosol particles sampled from southern African burning sources during the SAFARI 2000 mission, which included tar balls and soot, as well as mixed particles. While tar balls and soot were found to be hydrophobic, mixed particles and particles with inorganic coatings showed significantly enhanced hygroscopicity. A similar conclusion about the effect of inorganic material substantially increasing the hygroscopicity of smoke from Siberian fires was also reached by Popovicheva et al. (2016). Further, Vakkari et al. (2014) found that the hygroscopicity of smoke particles, again sampled from South African biomass burning areas, can increase rapidly within the first 2-4 hours due to oxidation and secondary aerosol formation. Aging and further oxidation of the smoke particles as they are transported to vast distances over the ocean may lead to further water uptake.

To our knowledge, this is the first report of a change in size distribution of smoke particles in this area far from the source regions. This is an important result, insofar as the aerosol indirect effect depends strongly on the size of the particles. The enhanced moisture associated with the smoke particles may also be important for radiative forcing and leads to a cooling in September-October in this area (Adebiyi et al., 2015). Therefore, this finding needs to be explored further using field missions as well as with satellite data. In fact, a major field mission, ORACLES, is currently studying the aerosol and cloud properties over this very region, and the ORACLES measurements should provide a wealth of resources to validate the results presented here.

5. Acknowledgements:

The CALIPSO aerosol and cloud profile data as well as the CATS lidar data are available at the NASA Langley Research Center Atmospheric Science Data Center. The MERRA 2 wind data were taken from the MERRA-2 Giovanni instance.

6. References:

Achtemeier, G. L.(2006): Measurements of moisture in smoldering smoke and implications for fog, Int. J. Wildland Fire, 15, 517-525.

Adebiyi, A. A. et al. (2015), The convolution of dynamics and moisture with the presence of shortwave absorbing aerosols over the Southeast Atlantic, J. Clim., 28, 1997-2024, doi:10.1175/J-CLI-D-14-00352.1.

Bibi, H., K. Alam and S. Bibi, (2016): "In-depth discrimination of aerosol types using multiple clustering techniques over four locations in Indo-Gangetic plains", Atmos. Res., **181**, 106-114, doi:10.1016/j.atmosres.2016.06.017.

Bond, T. C. et al. (2013), Bounding the role of black carbon in the climate system: A scientific assessment, J. Geophys. Res., 118, 5380-5552, doi:10.1002/jgrd.50171.

Burton, S. P., et al. (2013), Aerosol Classification from Airborne HSRL and Comparisons with the CALIPSO Vertical Feature Mask. Atmos. Meas. Tech., **6**, 1397-1412.

Chand, D. et al. (2008): Quantifying above-cloud aerosol using spaceborne lidar for improved understanding of cloudy-sky direct climate forcing, J. Geophys. Res., **113**, D13206, doi:10.1029/007JD009433.

Chand, D., et al. (2009): Satellite-derived direct radiative effect of aerosols dependent on cloud cover, Nature Geosc., **2**, 181-184,doi:10.1038/NGE0437.

Clements, C. B., Potter, B. E., and Zhong, S. (2006).: In situ measurements of water vapor, heat, and CO2 fluxes within a prescribed grass fire, Int. J. Wildland Fire, 15, 299-306.

Getzewich, B. J., et al. (2015): “CALIOP Calibration: Version 4.0 Algorithm Updates”, The 27th International Laser Radar Conference (ILRC 27), EPJ Web of Conferences, **119**, 04013, doi:10.1051/epjconf/201611904013.

Intergovernmental Panel on Climate Change, IPCC, (2013), Climate Change 2013: The physical science basis. The contribution of working group I to the Fifth Assessment Report of the Intergovernmental Panel on Climate Change.

Liu, Z., et al. (2009): “The CALIPSO Lidar Cloud and Aerosol Discrimination: Version 2 Algorithm and Initial Assessment of Performance”, J. Atmos. Oceanic Technol., 26, 1198–1213, doi:10.1175/2009JTECHA1229.1.

Midzak, N. et al. (2017), Determining smoke particle sphericity using CATS data, paper presented at the 97th Annual Meeting of the American Meteorological Society, Seattle, Jan 22-27, 2017.

Mielonen, T. et al. (2009). Comparison of CALIOP Level 2 aerosol subtypes to aerosol types derived from AERONET inversion data. Geophys. Res. Lett., 36, L18804.

Misra, A. K. et al. (2013). Study of MPLNET-derived aerosol climatology over Kanpur, India and validation of CALIPSO Level 2 version 3 backscatter and extinction products. J. Atmos. Oceanic Technol., **29**, 1285–1294.

Omar, A. et al. (2009), The CALIPSO automated aerosol classification and lidar ratio selection algorithm, J. Atmos. Oceanic Technol., 26, 1994-2014.

Popovicheva, O. B., et al. (2016), Small-scale study of Siberian biomass burning: II. Smoke hygroscopicity Aerosol and Air Quality Res., 16, 1558-1568.

Radke, L. F. et al., (1995), Effects of aging on the smoke from a large forest fire, Atmos. Res, 38, 315-332.

Randles, C. A. et al., (2016), The MERRA-2 aerosol assimilation, NASA/TM–2016-104606 / Vol. 45, vol. 45, ed. R. D. Koster.

Reid, J. S. et al. (2005), A review of biomass burning emissions part III. Intensive optical properties of biomass burning particles, Atmos. Chem. Phys., 5, 827-849.

Saide, P. E. (2015): Central American biomass burning smoke can increase tornado severity in the U.S, Geophys. Res. Lett., **42**, 956–965, doi:10.1002/2014GL062826.

Semeniuk, T. A., et al. (2007), Hygroscopic behavior of aerosol particles from biomass fires using environmental transmission electron microscopy, J. Atmos. Chem., 56, 259-273.

Vakkari, V., et al. (2014), Rapid changes in biomass burning aerosols by atmospheric oxidation, Geophys. Res. Lett., 41, 2644–2651, doi:10.1002/2014GL059396.

Van der Werf, G. R., et al. (2010), Global fire emissions and the contribution of deforestation, savanna, forest, agricultural, and peat fires (1997-2009), Atmos. Chem. Phys., 10, 11707-11735.

Vaughan, M., et al. (2009): "Fully Automated Detection of Cloud and Aerosol Layers in the CALIPSO Lidar Measurements", J. Atmos. Oceanic Technol., 26, 2034–2050, doi: 10.1175/2009JTECHA1228.1.

Winker, D. M. et al., (2009), Overview of the CALIPSO mission and CALIOP data processing algorithms, J. Atmos. Oceanic Technol., 26, 2310-2323.

Yorks, J. E. et al. (2016), An overview of the CATS Level 1 processing algorithms and data products, Geophys. Res. Lett., 43, 4632–4639, doi:10.1002/2016GL068006.

Zuidema, P. et al., (2016): Smoke and Clouds above the Southeast Atlantic: Upcoming Field Campaigns Probe Absorbing Aerosol's Impact on Climate, BAMS, 97, 1131–1135, doi:10.1175/BAMS-D-15-00082.1.